

PCCP

Accepted Manuscript



This is an *Accepted Manuscript*, which has been through the Royal Society of Chemistry peer review process and has been accepted for publication.

Accepted Manuscripts are published online shortly after acceptance, before technical editing, formatting and proof reading. Using this free service, authors can make their results available to the community, in citable form, before we publish the edited article. We will replace this *Accepted Manuscript* with the edited and formatted *Advance Article* as soon as it is available.

You can find more information about *Accepted Manuscripts* in the [Information for Authors](#).

Please note that technical editing may introduce minor changes to the text and/or graphics, which may alter content. The journal's standard [Terms & Conditions](#) and the [Ethical guidelines](#) still apply. In no event shall the Royal Society of Chemistry be held responsible for any errors or omissions in this *Accepted Manuscript* or any consequences arising from the use of any information it contains.

ARTICLE

Density functional theory study on boron- and phosphorus-doped hydrogen-passivated silicene

Cite this: DOI: 10.1039/x0xx00000x

Received 00th January 2012,
Accepted 00th January 2012

DOI: 10.1039/x0xx00000x

www.rsc.org/nanoscale

Xiaodong Pi,^a Zhenyi Ni,^a Yong Liu,^a Zhichao Ruan,^b Mingsheng Xu^c and Deren Yang^{*a}

When silicene is passivated by hydrogen, a bandgap occurs so that it becomes a semiconductor. Analogous to all the other semiconductors, doping is highly desired to realize the potential of hydrogen-passivated silicene (H-silicene). In the frame work of density functional theory (DFT), we have studied the doping of H-silicene with boron (B) and phosphorus (P). The concentration of B or P ranges from 1.4% to 12.5%. It is found that the doping of B or P enables the indirect-bandgap H-silicene to be a semiconductor with a direct bandgap. With the increase of the concentration of B or P, both the valence band and conduction band shift to lower energies, while the bandgap decreases. Both B and P doping lead to the decrease of the effective mass of holes and electrons in H-silicene. For both B- and P-doped H-silicene a subband absorption peak may appear, which blueshifts with the increase of the dopant concentration.

Introduction

Silicene, a novel two-dimensional graphene-like analogue for silicon (Si), has attracted great interests since it was successfully synthesized a few years ago.¹⁻⁶ Silicene owns a series of fascinating characteristics such as massless Dirac Fermions, quantum Hall effect and compatibility with Si-based nanoelectronics.⁷⁻¹¹ It is now quite compelling that silicene may open a new path for the development of next-generation devices.¹²⁻¹⁴ Similar to graphene, silicene is a semimetal without a bandgap. To realize the full potential of silicene in all kinds of device structures, it is widely believed that a bandgap should be generated for silicene.¹⁴⁻¹⁹ Up to now, hydrogenation has been an effective means to cause silicene to have a bandgap.²⁰⁻²⁴ It has been shown that hydrogenated silicene (H-silicene) is an indirect-bandgap semiconductor. Its bandgap is ~ 3.8 eV.²⁰ Since density functional theory (DFT) usually underestimates the bandgap of a semiconductor, the bandgap of H-silicene reported in the work carried out in the framework DFT with local density approximation (LDA) or generalized gradient approximation (GGA) is often ~ 2.2 eV.²⁰⁻²²

It is well known that semiconductors need to be doped for a variety of applications. As a novel semiconductor, H-silicene should also be doped to advance the development of H-silicene-based devices.²⁵⁻²⁷ For all kinds of semiconducting Si materials such as bulk Si,^{28, 29} Si nanowires^{30, 31} and Si nanocrystals,³²⁻³⁵ B and P have been the most important *p*- and *n*-type dopants, respectively. One may expect that B and P may also effectively dope H-silicene. However, it is now not clear how B and P exactly influence the electronic and optical properties of H-silicene when they are doped into H-silicene.

In this work, we investigate the electronic and optical properties of B- and P-doped H-silicene within the frame work of DFT. The band structures and optical absorption are calculated for B- and P-doped H-silicene with the dopant concentration ranging from 1.4% to 12.5%. It is found that the doping of B or P enables the indirect-bandgap H-silicene to be a semiconductor with a direct bandgap. In the meantime, the effective mass of holes or electrons in H-silicene may be reduced by doping. Interestingly, for both B- and P-doped H-silicene the effective mass of holes is always smaller than that of electrons. Finally we find that for both B- and P-doped H-silicene, a subband absorption peak may appear in the low energy region, which blueshifts with the increase of the dopant concentration. The interband absorption shows akin tendency for both B- and P-doped H-silicene.

Model and method

Figure 1 representatively shows an optimized structure of B- or P-doped H-silicene with top and side views. A $6 \times 6, 4 \times 4, 3 \times 3$, or 2×2 H-silicene supercell is constructed with one Si atom replaced by a B or P atom. This causes the concentration of B or P in H-silicene to be 1.4%, 3.1%, 5.6% or 12.5%, respectively. The distance between two adjacent H-silicene layers in each model is set as 20 Å to avoid image-image interaction. We should note that B and P atoms may form a variety of atomic configurations such as aggregates when their concentrations are rather high, as demonstrated by Yang et al³⁶ in their work on chlorine-passivated graphene. In this work we have avoided extensive investigation on the relative positions of dopants in H-silicene due to the constraint of our computational capacity. All the calculations of energy,

electronic and optical properties are performed by DFT, which is implemented in the Vienna *ab initio* simulation package (VASP) with the projector-augmented wave (PAW) method.^{37, 38} The Perdew-Burke-Ernzerhof (PBE) correlation exchange functional at the GGA level is adopted. The two-dimensional Brillouin zone is sampled with a Γ -centered ($11 \times 11 \times 1$) Monkhorst-Pack k-point grid in structural relaxation calculations.³⁹ All the calculations are carried out until the change in energy and the force on each atom are less than 1×10^{-6} eV per cell and 1×10^{-5} eV/Å, respectively. Please note that DFT calculations usually underestimate the bandgaps of semiconductors by $\sim 1 - 2$ eV because of quasiparticle and excitonic effects.^{40, 41} However, the relative order for the bandgaps is not affected by the underestimation.⁴⁰

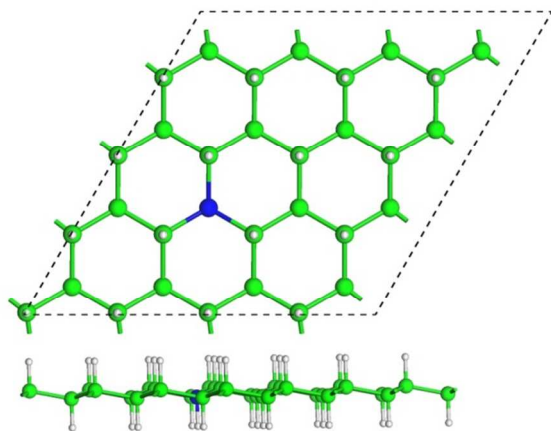


Fig. 1 Optimized structure of 4×4 H-silicene doped with B/P at the concentration of 3.1%. Both top and side views of the doped H-silicene are shown. Si, H and B/P atoms are denoted by green, white and blue balls, respectively. The unit cell of the structure is indicated by dashed lines.

The optical absorption of an undoped or P-doped H-silicene is derived from the in-plane frequency (ω)-dependent dielectric function ($\epsilon(\omega)$). The imaginary part of $\epsilon(\omega)$ is calculated by a summation over empty conduction band states using the equation:⁴²

$$\epsilon_{\alpha\beta}^i(\omega) = \frac{4\pi^2 e^2}{\Omega} \lim_{q \rightarrow 0} \frac{1}{q^2} \sum_{f,i,k} 2W_{\mathbf{k}} \delta(\epsilon_{f\mathbf{k}} - \epsilon_{i\mathbf{k}} - \omega) \times \langle u_{f\mathbf{k}+\mathbf{e}_{\alpha}q} | u_{i\mathbf{k}} \rangle \langle u_{f\mathbf{k}+\mathbf{e}_{\beta}q} | u_{i\mathbf{k}} \rangle^* \quad (1)$$

where the index α or β refers to one Cartesian component of the 3×3 Cartesian tensor; i and f refer to the initial and final electron transition states, respectively; Ω is the volume of the primitive cell; $u_{i\mathbf{k}}$ ($u_{f\mathbf{k}}$) is the cell's periodic part of the orbitals at the k-point \mathbf{k} ; \mathbf{e} is the unit vector for each of the three Cartesian directions. The optical absorption in an isolated sheet is then obtained by using⁴³

$$A(\omega) = \frac{\omega}{c} L \cdot \epsilon^i(\omega), \quad (2)$$

where c is the speed of light, L is the distance between adjacent atomic layers. Here only in-plane wave vectors are considered. A ($11 \times 11 \times 1$) Monkhorst-Pack k-point grid is adopted and the number of bands is doubled with respect to the VASP default in the calculation to get a reasonable result. However, we should note that the final state in equation (1) should be completely

empty. If a band is partially filled with electrons, it can only be regarded as the initial state of the transition of an electron, rather than the final state of the transition of an electron.⁴²

Results and discussion

Figure 2 shows the band structures of B- or P-doped H-silicene. It is seen that when H-silicene is doped with B or P, it becomes a direct-bandgap semiconductor. Both the valence band maximum (VBM) and conduction band minimum (CBM) of B- or P-doped H-silicene appear at the Γ point. Please note that although the bands are folded when a large supercell is used to calculate the band structure of B- or P-doped H-silicene, the valence band and conduction band of doped H-silicene are not affected by the band-folding. This is because no folding points appear in these bands at the high symmetry point of Γ , M or K. For B (P)-doped H-silicene, the Fermi energy level enters the valence (conduction) band when the concentration of B (P) is 1.4% (Fig. 2 (a) and (e)). This indicates that H-silicene is heavily doped even if the lowest dopant concentration of 1.4% is used in the current work. With the increase of the concentration of B up to 12.5%, the difference in energy between the Fermi energy level and VBM of B-doped H-silicene becomes larger (i.e., 0.02 \rightarrow 0.48 eV). The difference in energy between the Fermi energy level and CBM changes from 0.13 to 0.79 eV when the concentration of P increases from 1.4% to 12.5%. It has been shown in previous work that H-silicene is an indirect-bandgap semiconductor.²⁰⁻²² The VBM of H-silicene appears at the Γ point, while the CBM appears at the M point. The difference in energy between direct-bandgap and indirect-bandgap of H-silicene is ~ 0.21 eV.²¹ For H-silicene doped with B at the concentrations of 1.4% - 12.5%, the energies of the direct bandgap and indirect bandgap are quite close (< 0.47 eV). However, the difference in energy between the direct bandgap and indirect bandgap of P-doped H-silicene varies from 0.13 to 0.80 eV when the concentration of P increases from 1.4% to 12.5%. This implies that P doping more seriously modifies the band structure of H-silicene.

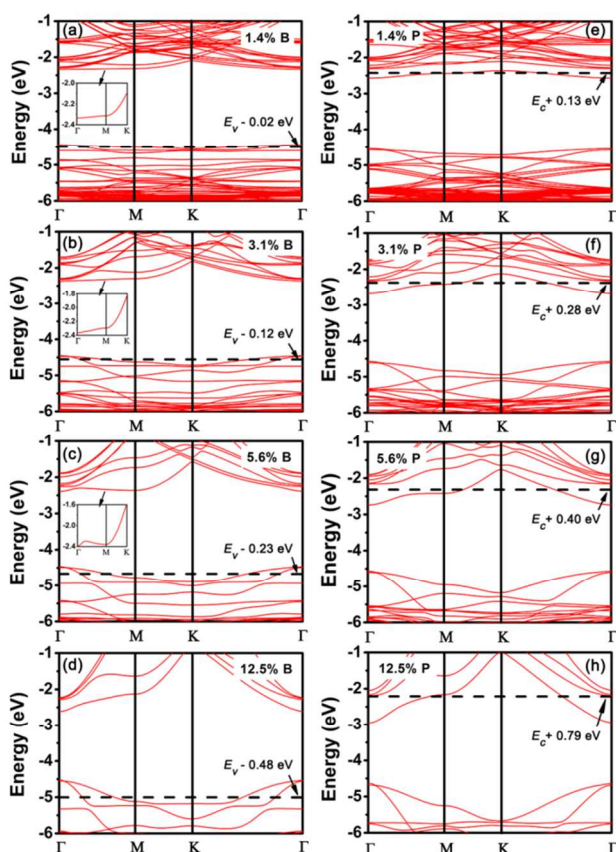


Fig. 2 Band structure of H-silicene doped with B at the concentration of (a) 1.4%, (b) 3.1%, (c) 5.6% or (d) 12.5%. Band structure of H-silicene doped with P at the concentration of (e) 1.4%, (f) 3.1%, (g) 5.6% or (h) 12.5%. The Fermi energy level is indicated by a horizontal dashed line. The difference in energy between the Fermi energy level and VBM (CBM) of B (P)-doped H-silicene is indicated. The conduction band of H-silicene doped with B at the concentration of (a) 1.4%, (b) 3.1% or (c) 5.6% is enlarged along $\Gamma \rightarrow K$ to facilitate the visualization of the direct bandgap.

The variations of the VBM, CBM and Fermi energy with the dopant concentration for B- or P-doped H-silicene are shown in figure 3 (a) and (b). We can see that the VBM, CBM and Fermi energy all decrease as the concentration of B increases (Fig. 3(a)). However, the CBM more significantly decreases than the VBM, resulting in the decrease of the bandgap of B-doped H-silicene from 2.10 to 1.92 eV when the concentration of B increases from 1.4% to 12.5% (Fig. 3 (c)). For P-doped H-silicene, with the increase of concentration of P, both the CBM and VBM decrease, while the Fermi energy increases. Since the CBM more significantly decreases than the VBM, the bandgap of P-doped H-silicene decreases from 1.97 to 1.69 eV when the concentration of P increases from 1.4% to 12.5% (Fig. 3 (d)). It is clear that P slightly more seriously reduces the bandgap of H-silicene than B does when they are doped with the same concentration (Fig. 3 (c) and (d)). Due to the Burstein-Moss effect,⁴⁴ an effective bandgap that corresponds to absorption onset is always larger than the bandgap for a heavily doped semiconductor. The effective bandgap is in fact the difference between the CBM (VBM) and the first energy level (above) the Fermi energy level for B (P)-doped H-silicene. The changes of the effective bandgap with the dopant concentration

for B- and P-doped H-silicene are shown in figure 3 (c) and (d), respectively. In contrast to the bandgap, the effective bandgap increases as the dopant concentration increases for B- or P-doped H-silicene. In the meantime, we may notice that the effective bandgap of P-doped H-silicene is smaller than that of B-doped H-silicene when the dopant concentration is the same.

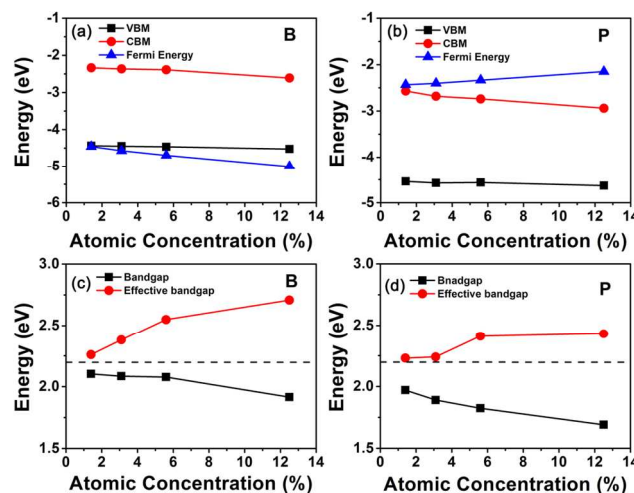


Fig. 3 Variation of the valence band maximum (VBM), conduction band minimum (CBM) and Fermi energy with the dopant concentration for H-silicene doped with (a) B or (b) P. Variation of the bandgap and effective bandgap with the dopant concentration for H-silicene doped with (c) B or (d) P. The bandgap of undoped H-silicene (2.2 eV) is indicated by a horizontal dashed line.

Although H-silicene has a bandgap, the linear Dirac cone of the original silicene disappears. Therefore, the effective mass of holes or electrons in H-silicene is quite large ($m_e^{\Gamma\Gamma} = 2.63m_0$, $m_e^{\Gamma K} = 0.19m_0$, $m_h^{\Gamma M} = 0.81m_0$ and $m_h^{\Gamma K} = 0.78m_0$, where m_0 is the free electron mass)²¹. Our current work demonstrates that the effective mass of holes or electrons in H-silicene may decrease to some degree after doping. We have calculated the effective mass m^* of holes (electrons) at the VBM (CBM) for H-silicene doped with B or P by using⁴⁵

$$m^* = \hbar^2 \left(\frac{d^2E}{dk^2} \right)^{-1}. \quad (3)$$

When the slightly anisotropic dispersion of E for the VBM and CBM at the Γ point is ignored, the average values of the effective mass of holes (m_h^*) or electrons (m_e^*) in H-silicene doped with B and P with concentrations of 1.4% - 12.5% are readily obtained, as shown in figure 4. For B-doped H-silicene, both m_h^* and m_e^* decrease as the concentration of B increases from 1.4% to 5.6%. When the concentration of B further increases to 12.5%, the m_h^* and m_e^* increase again. The values of m_h^* and m_e^* are the smallest for B-doped H-silicene when the concentration of B is 5.6% ($m_h^* \approx 0.19 m_0$, $m_e^* \approx 0.19 m_0$). This indicates that a relatively larger carrier mobility may be achieved when the concentration of B is 5.6%. For P-doped H-silicene, m_e^* monotonously decreases as the concentration of P increases, while m_h^* increases when the concentration of P increases from 1.4% to 5.6% and decreases as the concentration of P further increases. The smallest values of m_h^* and m_e^* can be obtained for P-doped H-silicene when the concentration of P is 12.5% ($m_h^* \approx 0.17 m_0$, $m_e^* \approx 0.21 m_0$) in the current work. The

values of m_h^* and m_e^* of P-doped H-silicene are smaller than those of B-doped H-silicene when the dopant concentration is the same, except for the case of the dopant concentration of 5.6%. Interestingly, the value of m_h^* is always smaller than that of m_e^* for both B- and P-doped H-silicene with the same dopant concentration. This is in contrast to what occurs for bulk silicon. If we assume that the average scattering time of holes is similar to that of electrons, the carrier mobility of holes should be larger than that of electrons in B- or P-doped H-silicene.

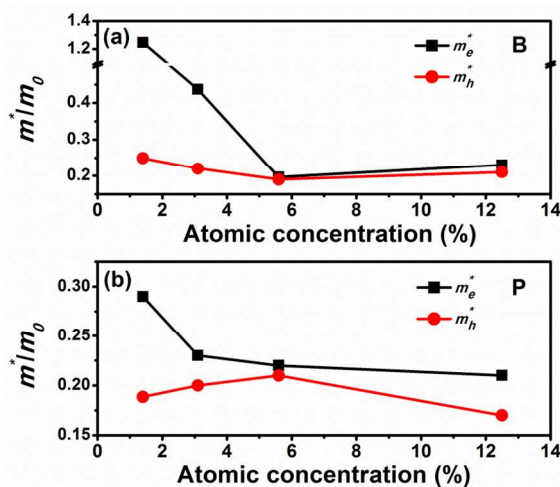


Fig. 4 Variation of the effective mass of electrons (m_e^*) and holes (m_h^*) with the dopant concentration for H-silicene doped with (a) B or (b) P.

Now we move to discuss the optical absorption of doped H-silicene. Figure 5 (a) shows the absorption spectra of undoped and P-doped H-silicene. For undoped H-silicene, the absorption spectrum shows an absorption onset at ~ 2.18 eV, which is consistent with the bandgap of H-silicene. For P-doped H-silicene, a subband absorption peak occurs in the low-energy region. The energy of the subband absorption is shown in figure 5 (b). The subband absorption results from electronic transition involving P-induced energy levels near the CBM. The optical absorption feature of P-doped H-silicene can be interpreted by the eigenvalues $E_n(\mathbf{k})$ of the Kohn-Sham equation in the Brillouin zone. The absorption peak occurs at a critical point, where $E_{n'}(\mathbf{k})$ and $E_n(\mathbf{k})$ have the same slope, i.e.,⁴³

$$\nabla[E_{n'}(\mathbf{k}) - E_n(\mathbf{k})] = 0, \quad (4)$$

where the indices n and n' indicate the initial and final electron transition states, respectively. The subband absorption peak of P-doped H-silicene corresponds to the transition of an electron from the CBM to the first energy level above the Fermi energy level at the Γ point ($T_1 \rightarrow T_2$), as shown in figure 6. In addition to the subband absorption, band-edge absorption can also be observed for P-doped H-silicene in the high energy region. The band-edge absorption onset corresponds to the transition of an electron from the VBM to the first energy level above the Fermi energy level at the Γ point ($T_0 \rightarrow T_2$), which has also been indicated in figure 6. The energy for the $T_0 \rightarrow T_2$ transition is actually equal to the effective bandgap (Fig. 3 (d)). However, for B-doped H-silicene, because of the limitation of equation (1) the partially filled valence band cannot be regarded as the final state of the transition of an electron. This disables us to calculate the optical absorption of B-doped H-silicene.

Nevertheless, we may figure out the subband absorption peak and band-edge absorption onset through the band structure of B-doped H-silicene, analogous to what is learnt in the case of P-doped H-silicene.

Figure 5 (b) shows the variation of the subband absorption peak with the dopant concentration for B- or P-doped H-silicene. It is seen that for both B- and P-doped H-silicene the subband absorption peak blueshifts as the dopant concentration increases. This results from the fact that the Fermi energy level more deeply enters the valence (conduction) band of doped H-silicene as the concentration of B (P) increases (Fig. 2). The energy of the subband absorption increases from 0.16 (0.26) to 0.79 (0.75) eV when the concentration of B (P) increases from 1.4% to 12.5%. For a dopant concentration between 1.4% and 5.6% the Fermi energy level more deeply enters the conduction band of P-doped H-silicene than it enters the valence band of B-doped H-silicene. Therefore, the subband absorption peak of P-doped H-silicene blueshifts compared with that of B-doped H-silicene when B and P are doped with the same concentration in the range from 1.4% to 5.6%. However, the subband absorption of B- and P-doped H-silicene peaks at similar energies when B and P are doped with the rather high concentration of 12.5%. This is because the decrease of the first energy level below the Fermi energy level of B-doped H-silicene is more than the increase of the first energy level above the Fermi energy level of P-doped H-silicene when the dopant concentration is 12.5%. It is clear that the optical absorption is enhanced in the energy region from 0.2 to 0.8 eV for B- or P-doped H-silicene compared with that for undoped H-silicene. Given the fact that GGA calculations may underestimate the bandgap of B- or P-doped H-silicene by $\sim 1-2$ eV, the enhanced optical absorption should be helpful if solar cells are prepared by using doped H-silicene.

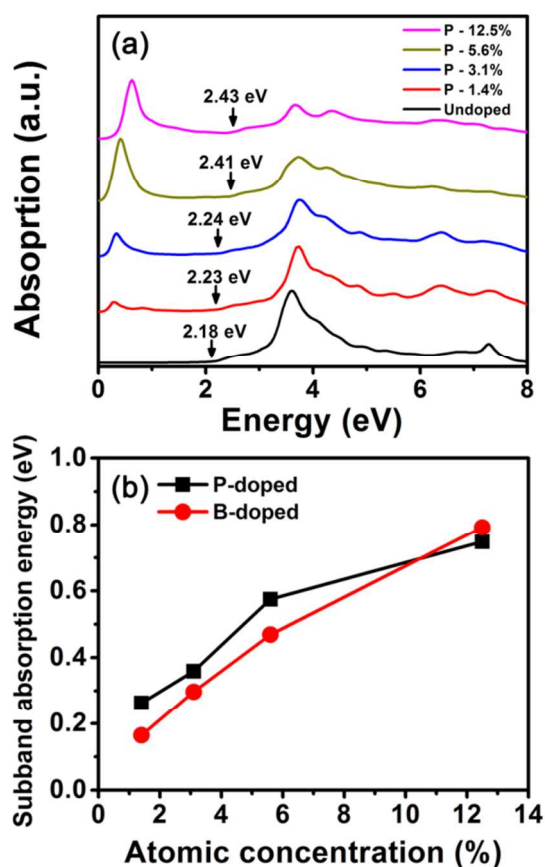


Fig. 5 (a) Optical absorption spectra of undoped H-silicene and H-silicene doped with P at the concentration of 1.4%, 3.1%, 5.6% or 12.5%. The band-edge absorption onset is indicated by an arrow. (b) Variation of the energy of the subband absorption of B- or P-doped H-silicene with the dopant concentration.

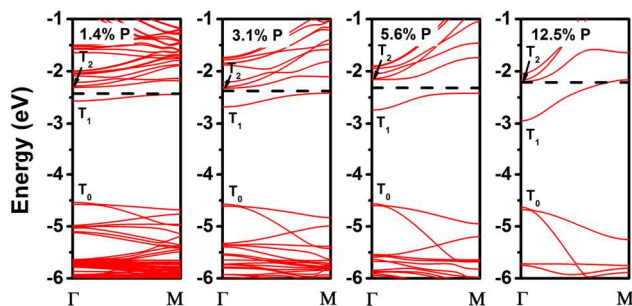


Fig. 6 Part of the band structure of H-silicene doped with P at the concentration of 1.4%, 3.1%, 5.6% or 12.5%. The Fermi energy level is indicated by a horizontal dashed line. The electron transitions that correspond to interband absorption onset and sub-band absorption peak are shown as $T_0 \rightarrow T_2$ and $T_1 \rightarrow T_2$, respectively.

Conclusion

We have investigated the electronic and optical properties of B- or P-doped H-silicene. It is found that the doping of B or P enables the indirect-bandgap H-silicene to be a direct bandgap semiconductor. The Fermi energy level enters the valence (conduction) band of B (P)-doped H-silicene when the dopant

concentration varies from 1.4% to 12.5%. The effective mass of holes and electrons in H-silicene can be reduced by doping. In contrast to traditional bulk silicon, the value of m_h^* is always smaller than that of m_e^* for both B- and P-doped H-silicene. With the increase of the concentration of B or P, both the CBM and VBM shift to lower energies. However, the CBM more significantly decreases than the VBM, resulting in the decrease of the bandgap of B- or P-doped H-silicene. For both B- and P-doped H-silicene a subband absorption peak appears, which blueshifts with the increase of the dopant concentration. The theoretical insights gained in the current work should help to advance the development of silicene-based devices in the future. For instance, the direct bandgap B- or P-doped H-silicene may not only enable the preparation of solar cells by using doped H-silicene, but also render promise for the use of doped H-silicene in light-emitting devices.

Acknowledgements

Shanghai Supercomputer Center is acknowledged for providing computation resources. This work is mainly supported by the 973 program (Grant No. 2013CB632101) and the NSFC for excellent young researchers (Grant No. 61222404). Partial support is provided by the Fundamental Research Funds for the Central Universities (2014XZZX003-09).

Notes and references

- ^a State Key Laboratory of Silicon Materials and Department of Materials Science and Engineering, Zhejiang University, Hangzhou, Zhejiang 310027, China.
^b Department of Physics, Zhejiang University, Hangzhou, Zhejiang 310027, China.
^c Department of Polymer Science and Engineering, Hangzhou, Zhejiang 310027, China.

† Footnotes should appear here. These might include comments relevant to but not central to the matter under discussion, limited experimental and spectral data, and crystallographic data.

Electronic Supplementary Information (ESI) available: [details of any supplementary information available should be included here]. See DOI: 10.1039/b000000x/

- P. Vogt, P. De Padova, C. Quaresima, J. Avila, E. Frantzeskakis, M. C. Asensio, A. Resta, B. Ealet and G. Le Lay, *Phys. Rev. Lett.*, 2012, **108**, 155501.
- B. Feng, Z. Ding, S. Meng, Y. Yao, X. He, P. Cheng, L. Chen and K. Wu, *Nano Lett.*, 2012, **12**, 3507-3511.
- L. Chen, C.-C. Liu, B. Feng, X. He, P. Cheng, Z. Ding, S. Meng, Y. Yao and K. Wu, *Phys. Rev. Lett.*, 2012, **109**, 056804.
- H. Jamgotchian, Y. Colignon, N. Hamzaoui, B. Ealet, J. Y. Hoarau, B. Aufray and J. P. Biberian, *J. Phys. Cond. Matt.*, 2012, **24**, 172001.
- P. De Padova, C. Ottaviani, C. Quaresima, B. Olivieri, P. Imperatori, E. Salomon, T. Angot, L. Quagliano, C. Romano, A. Vona, M. Muniz-Miranda, A. Generosi, B. Paci and G. Le Lay, *2D Mater.*, 2014, **1**, 021003.
- M. Xu, T. Liang, M. Shi and H. Chen, *Chem. Rev.*, 2013, **113**, 3766-3798.

7. A. Kara, H. Enriquez, A. P. Seitsonen, L. C. L. Y. Voon, S. Vizzini, B. Aufray and H. Oughaddou, *Surf. Sci. Rep.*, 2012, **67**, 1.
8. H. Okamoto, Y. Sugiyama and H. Nakano, *Chem. Eur. J.*, 2011, **17**, 9864-9887.
9. C.-C. Liu, W. Feng and Y. Yao, *Phys. Rev. Lett.*, 2011, **107**, 076802.
10. J. Gao, J. Zhang, H. Liu, Q. Zhang and J. Zhao, *Nanoscale*, 2013, **5**, 9785-9792.
11. B. Huang, H.-X. Deng, H. Lee, M. Yoon, B. G. Sumpter, F. Liu, S. C. Smith and S.-H. Wei, *Phys. Rev. X*, 2014, **4**, 021029.
12. K. J. Koski and Y. Cui, *ACS Nano*, 2013, **7**, 3739.
13. D. Chiappe, C. Grazianetti, G. Tallarida, M. Fanciulli and A. Molle, *Adv. Mater.*, 2012, **24**, 5088-5093.
14. Z. Ni, H. Zhong, X. Jiang, R. Quhe, G. Luo, Y. Wang, M. Ye, J. Yang, J. Shi and J. Lu, *Nanoscale*, 2014, **6**, 7609-7618.
15. R. Quhe, R. Fei, Q. Liu, J. Zheng, H. Li, C. Xu, Z. Ni, Y. Wang, D. Yu, Z. Gao and J. Lu, *Sci. Rep.*, 2012, **2**, 853.
16. Z. Ni, Q. Liu, K. Tang, J. Zheng, J. Zhou, R. Qin, Z. Gao, D. Yu and J. Lu, *Nano Lett.*, 2012, **12**, 113-118.
17. N. D. Drummond, V. Zólyomi and V. I. Fal'ko, *Phys. Rev. B*, 2012, **85**, 075423.
18. Y. Liang, V. Wang, H. Mizuseki and Y. Kawazoe, *J. Phys. Cond. Matt.*, 2012, **24**, 455302.
19. J. Sivek, H. Sahin, B. Partoens and F. Peeters, *Phys. Rev. B*, 2013, **87**, 085444.
20. M. Houssa, E. Scalise, K. Sankaran, G. Pourtois, V. V. Afanas'ev and A. Stesmans, *Appl. Phys. Lett.*, 2011, **98**, 223107.
21. R. Wang, X. Pi, Z. Ni, Y. Liu and D. Yang, *submitted*.
22. P. Zhang, X. D. Li, C. H. Hu, S. Q. Wu and Z. Z. Zhu, *Phys. Lett. A*, 2012, **376**, 1230-1233.
23. Y. Ding and Y. Wang, *Appl. Phys. Lett.*, 2012, **100**, 083102.
24. V. Zólyomi, J. R. Wallbank and V. I. Fal'ko, *2D Mater.*, 2014, **1**, 011005.
25. H.-X. Luan, C.-W. Zhang, F.-B. Zheng and P.-J. Wang, *J. Phys. Chem. C*, 2013, **117**, 13620-13626.
26. F.-B. Zheng, C.-W. Zhang, P.-J. Wang and S.-S. Li, *J. Appl. Phys.*, 2013, **113**, 154302.
27. J.-M. Zhang, W.-T. Song, K.-W. Xu and V. Ji, *Comp. Mater. Sci.*, 2014, **95**, 429.
28. R. R. Troutman, G. D. Ji and W. H. Lu, *Latch-up in CMOS Technology: The problem and its Cure*, Kluwer Academic, Boston, 1986.
29. Y. H. Zeng, X. Y. Ma, J. H. Chen, W. J. Song, W. Y. Wang, L. F. Gong, D. X. Tian and D. R. Yang, *J. Appl. Phys.*, 2012, **111**, 033520.
30. O. Moutanabbir, D. Isheim, H. Blumtritt, S. Senz, E. Pippel and D. N. Seidman, *Nature*, 2013, **496**, 78-82.
31. S. Kim, J. S. Park and K. J. Chang, *Nano Lett.*, 2012, **12**, 5068-5073.
32. X. D. Pi, R. Gresback, R. W. Liptak, S. A. Campbell and U. Kortshagen, *Appl. Phys. Lett.*, 2008, **92**, 123102.
33. X. Pi and C. Delerue, *Phys. Rev. Lett.*, 2013, **111**, 177402.
34. X. D. Pi, *J. Nanomater.*, 2012, **2012**, 1-9.
35. S. Zhou, X. D. Pi, Z. Y. Ni, Q. B. Luan, Y. Y. Jiang, C. H. Jin, T. Nozaki and D. Yang, *Part. Part. Syst. Char.*, 2014, DOI: 10.1002/ppsc.201400103.
36. M. Yang, L. Zhou, J. Wang, Z. Liu and Z. Liu, *J. Phys. Chem. C*, 2012, **116**, 844-850.
37. P. E. Blöchl, *Phys. Rev. B*, 1994, **50**, 17953-17979.
38. G. Kresse and D. Joubert, *Phys. Rev. B*, 1999, **59**, 1758-1775.
39. H. J. Monkhorst and J. D. Pack, *Phys. Rev. B*, 1976, **13**, 5188-5192.
40. A. J. Williamson, J. C. Grossman, R. Q. Hood, A. Puzder and G. Galli, *Phys. Rev. Lett.*, 2002, **89**, 196803.
41. A. Puzder, A. J. Williamson, F. A. Reboredo and G. Galli, *Phys. Rev. Lett.*, 2003, **91**, 157405.
42. M. Gajdoš, K. Hummer, G. Kresse, J. Furthmüller and F. Bechstedt, *Phys. Rev. B*, 2006, **73**, 045112.
43. L. Matthes, P. Gori, O. Pulci and F. Bechstedt, *Phys. Rev. B*, 2013, **87**, 035438.
44. M. T. S., B. G. T. and E. B., *Semiconductor Opto-electronics*, 1973, Butterworths, London.
45. R. Wang, X. Pi, Z. Ni, Y. Liu, S. Lin, M. Xu and D. Yang, *Sci. Rep.*, 2013, **3**, 3507.